Journal of Engineering and Applied Sciences 12 (23): 7180-7188, 2017
ISSN: 1816-949X


# Dynamics of a Mobile Manipulator of 8 Degrees of Freedom for Inspection Tasks

C. Angie J. Valencia, Oscar F. Aviles and Mauricio F. Mauledoux
Mechatronics Engineering Program, Faculty of Engineering,
Militar Nueva Granada University, Bogota, Colombia

**Abstract:** Dynamics is an enormous field dedicated to the study of the forces required to cause movement. To accelerate a manipulator from an inert position, slide it with a constant speed of the end effector and finally decelerate it to a complete stop, whereby the joint actuators must apply a complex set of rotational moments functions. The exact form of the required functions of moment of rotation of an actuator depends on the kinematic and dynamic parameters of each one. A method for controlling a manipulator to follow a desired path involves calculating these functions using the dynamic equations of the manipulator's motion. On the other hand, for mobile robots, the dynamics allows determining the necessary torque required to reach the speeds in each wheel. In addition, it creates additional restrictions to the workspace and trajectories due to the consideration of masses and forces acting on the robotic platform. For the above, the present research describes the dynamic model for a hybrid platform composed of a manipulator arm of 5 degrees of freedom and a mobile platform of six wheels with traction in each of them.

**Key words:** Direct dynamic, inverse dynamic, wheels dynamic, generalize coordinates, degrees of freedom, manipulator robot, mobile robot

## INTRODUCTION

Most mobile robots have special characteristics that allow them to adapt to certain tasks such as the inspection and reconstruction of land (Campion *et al*., 1993). It is the definition of the tasks that determines the structural particularities of the robot, defined by the type of wheel or articulation as well as the system of traction and direction and the mechanical form of the robot which opens the way to specific the sensory characteristics of the robot (Williams *et al*., 2002; Jones *et al*., 1993). To achieve the reliability and maneuverability of the mechanism, the calculation of the dynamics underlying the mathematical formulations of the equations in motion between articular coordinates (robot end coordinates), their derivatives (velocity and acceleration), forces and pairs applied to the joints and robot parameters (masses, inertia, etc.), to relate the movement of the robot and the forces involved in it (Zoo and Bement, 1992).

There are two methods for calculating the mathematical models of the dynamics system: the Newton-Euler and the Euler-Lagrange formulation. These provide the same equations of motion in the mechanisms but from two different points of view. On the one hand Newton-Euler's approach is based on an iterative calculation of the balance of system forces by defining the linear and angular equations of motion of each link independently. While the Euler-Lagrange formulation bases its structure on the balance of system energies, it is posed as the difference between kinetic and potential energy. In this one can also be considered the effects of friction caused by the mechanical transmissions of the engines that propose the system as non-conservative (important consideration because the frictions can reach 25% of the torque required to move the manipulator) (Craige, 1989).

## MATERIALS AND METHODS

**Robotic manipulator dynamics:** For the development of the present work we consider the scheme of Fig. 1, where the structure of the mobile manipulator is specified. It should be considered that for the dynamic calculations of the mechanism a decoupling is contemplated between the mobile platform and the manipulator where by the frame of reference and movement of the manipulator is considered at the beginning of the kinematic chain but not as the set of global coordinates of the hybrid platform. For notation $s_{\theta 1} = \sin(\theta_1)$, $c_{\theta 1} = \cos(\theta_1)$, $s_{(\theta 1+\theta 2)} = \sin(\theta_1+\theta_2)$, $c_{\theta 1+\theta 2)} = \cos(\theta_1+\theta_2)$, $s_{(\theta 1+\theta 2+\theta 3)} = \sin(\theta_1+\theta_2+\theta_3)$, $c_{(\theta 1+\theta 2+\theta 3)} = \cos(\theta_1+\theta_2+\theta_3)$.

**Manipulator dynamics:** We will implement the lagrange formulation and the Rayleigh dissipation function that

**Corresponding Author:** C. Angie J. Valencia, Mechatronics Engineering Program, Faculty of Engineering, Militar Nueva Granada University, Bogota, Colombia

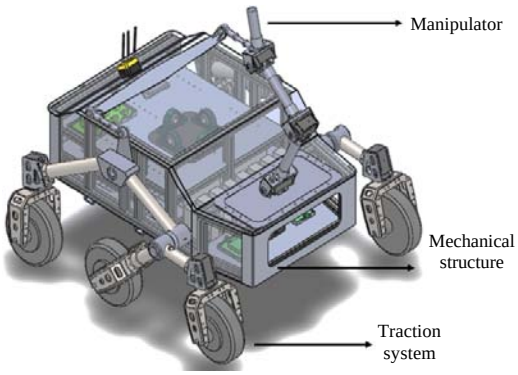


Fig. 1: Hybrid platform scheme

considers the friction effects already mentioned. Losses due to joint strikes as well as engine efficiency are neglected in the analysis of the Lagrange equation of motion. Finally, the manipulating mechanism of Fig. 2 is considered as a rigid system, concentrating the masses in the center of each link as is shown in Fig. 3.

To calculate the dynamics of the manipulator, it must be considered that there are two techniques for its calculation: direct and inverse.

**Inverse dynamics:** The dynamic model of the robotic arm of DOF is obtained by applying the Lagrangian motion equation defined by the Lagrangian of Eq. 1 with its motion equations given by Eq. 2:

$$L = K-U \tag{1}$$

$$\frac{d}{dt}\left[\frac{\partial L}{\partial \dot{q}_i}\right]-\left[\frac{\partial L}{\partial q_i}\right]+\left[\frac{\partial D}{\partial \dot{q}_i}\right]=\tau \tag{2}$$

Where:

K = The kinetic energy of the system
U = The potential energy
q = The generalized coordinates that describe the positions of the manipulator links of n DOF
$\dot{q}$ = Its derivative
$\tau$ = The generalized force associated with generalized coordinates
D = The Rayleigh dissipation function

$$D=\frac{1}{2}\left[b_i\times\dot{\delta}_i^2\right]$$

where, $\dot{\delta}_i$ the velocity difference through the viscous damper that can be expressed as a function of the generalized variables $\dot{q}_i$ (Ogata, 1987). The kinetic energy of the system is defined in Eq. 3 for rotational and

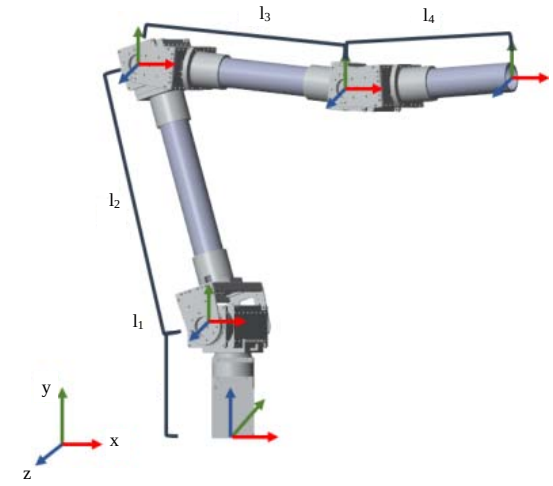


Fig. 2: Five DOF arm scheme

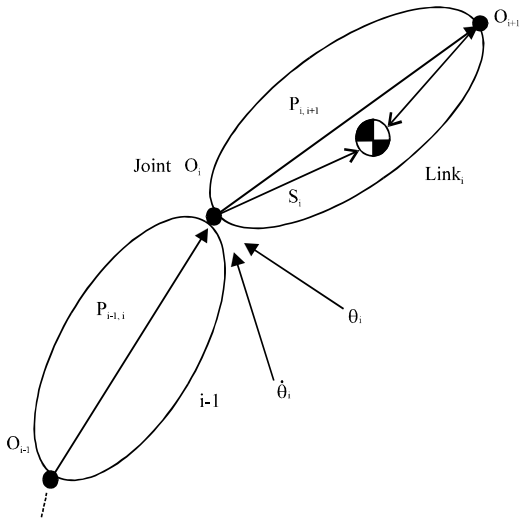


Fig. 3: Location of the centers of mass of the links

in Eq. 4 for linear. Where m is the mass of the element $\dot{\theta}_i$ and $\dot{v}_i$ are the rotational and linear velocities, respectively of the link I is the inertia of the element defined by $I = m.l_i^2$, y l is the length of the link:

$$K_R=\frac{1}{2}\times I_i\times\dot{\theta}_i^2 \tag{3}$$

$$K_L=\frac{1}{2}\times m_i\times v_i^2 \tag{4}$$

For the analysis of the articulation of the base we have Eq. 5 and 6 that describe the kinetic energy of the same:

$$K_b = \frac{1}{2} \times I_b \times \dot{\theta}_1^2 \quad (5)$$

$$I_b = \frac{1}{2} \times m_b \times r^2 \quad (6)$$

For this case, the potential energy is zero because there are no changes in height that generate motion in $\theta_1$. We proceed with the analysis of joint 1 of which we have the Eq. 7-11 to describe the kinetic energy and Eq. 12 for the potential energy:

$$K_1 = \frac{1}{2} \times m_1 \times v_1^2 + \frac{1}{2} \times I_1 \times \dot{\theta}_2^2 \quad (7)$$

$$v_1^2 = \dot{x}_1^2 + \dot{y}_1^2 \quad (8)$$

$$x_1 = \frac{l_1}{2} \times c_{\theta_2} \quad (9)$$

$$y = \frac{l_1}{2} \times s_{\theta_2} \quad (10)$$

$$I_1 = m_1 \times x_1^2 \quad (11)$$

$$p_1 = m_1 \times g \times \frac{l_1}{2} \times s_{\theta_2} \quad (12)$$

Then, we have for the joint 2 the kinetic energy is given by Eq. 13-17 while the potential energy is given by Eq. 18:

$$K_2 = \frac{1}{2} \times m_2 \times v_2^2 + \frac{1}{2} \times I_2 \times \dot{\theta}_3^2 \quad (13)$$

$$v_2^2 = \dot{x}_2^2 + \dot{y}_1^2 \quad (14)$$

$$x_2 = I_1 \times c_{\theta_2} + \frac{I_2}{2} \times c_{(\theta_2+\theta_3)} \quad (15)$$

$$y_2 = I_1 \times s_{\theta_2} + \frac{I_2}{2} \times s_{(\theta_2+\theta_3)} \quad (16)$$

$$I_2 = m_2 \times x_2^2 \quad (17)$$

$$p_2 = m_2 \times g \times I_1 \times s_{\theta_2} + m_2 \times g \times \frac{l_2}{2} \times s_{(\theta_2+\theta_3)} \quad (18)$$

For joint 3, the kinetic energy is given by Eq. 19-23 while the potential energy is given by Eq. 24:

$$K_3 = \frac{1}{2} \times m_3 \times v_3^2 + \frac{1}{2} \times I_3 \times \dot{\theta}_4^2 \quad (19)$$

$$v_3^2 = \dot{x}_3^2 + \dot{y}_3^2 \quad (20)$$

$$x_3 = l_1 \times c_{\theta_2} + l_2 \times c_{(\theta_2+\theta_3)} + \frac{l_3}{2} \times c_{(\theta_2+\theta_3+\theta_4)} \quad (21)$$

$$y_3 = l_1 \times s_{\theta_2} + l_2 \times s_{(\theta_2+\theta_3)} + \frac{l_3}{2} \times s_{(\theta_2+\theta_3+\theta_4)} \quad (22)$$

$$I_3 = m_3 \times x_3^2 \quad (23)$$

$$p_3 = m_3 \times g \times l_1 \times s_{\theta_2} + m_3 \times g \times l_2 \times s_{(\theta_2+\theta_3)} + m_3 \times g \times \frac{l_3}{2} \times s_{(\theta_2+\theta_3+\theta_4)} \quad (24)$$

Finally, for the gripper joint the kinetic energy is given by Eq. 25-29 while the potential energy is given by Eq. 30:

$$K_c = \frac{1}{2} \times m_c \times v_c^2 + \frac{1}{2} \times I_c \times \dot{\theta}_4^2 \quad (25)$$

$$v_c^2 = \dot{x}_c^2 + \dot{y}_c^2 \quad (26)$$

$$x_c = l_1 \times c_{\theta_2} + l_2 \times c_{(\theta_2+\theta_3)} + l_3 \times c_{(\theta_2+\theta_3+\theta_4)} \quad (27)$$

$$y_c = l_1 \times s_{\theta_2} + l_2 \times s_{(\theta_2+\theta_3)} + l_3 \times s_{(\theta_2+\theta_3+\theta_4)} \quad (28)$$

$$I_c = m_c \times x_c^2 \quad (29)$$

$$p_c = w_c \times g \times l_1 \times s_{\theta_2} + w_c \times g \times l_2 \times s_{(\theta_2+\theta_3)} + w_c \times g \times l_3 \times s_{(\theta_2+\theta_3+\theta_4)} \quad (30)$$

Returning to Eq. 1, the Lagrangian calculation is performed as shown in Eq. 31:

$$L = K_b + K_1 + K_2 + K_3 + K_c - p_b - p_{b1} - p_2 - p_3 - p_c \quad (31)$$

The lagrangian of Eq. 31 must be derived as shown in Eq. 2 for the calculation of the derivative for the generalized coordinate $\theta_1$ will be performed as an illustrative example. Therefore, in Eq. 32-34 the derivatives for the articulation of the base are shown as:

$$\frac{\partial L}{\partial \dot{q}_1} = m_3 \times \dot{\theta}_1 \times \left(l_2 \times c_{(\theta_2+\theta_3)} + l_1 \times c_{\theta_2} + \left(l_3 \times c_{(\theta_2+\theta_3+\theta_4)}\right)/2\right)^2 + \dot{\theta}_1 \times w_c \times \left(l_2 \times c_{(\theta_2+\theta_3)} + l_1 \times c_{\theta_2} + l_3 \times c_{(\theta_2+\theta_3+\theta_4)}\right)^2 + m_b \times r^2 \times \dot{\theta}_1 + \left(m_2 \times \dot{\theta}_1 \times \left(l_2 \times c_{(\theta_2+\theta_3)} + 2 \times l_1 \times c_{\theta_2}\right)^2\right)/4 + \left(l_1^2 \times m_1 \times \dot{\theta}_1 \times c_{\theta_2}^2\right)/4 \quad (32)$$

$$\frac{d}{dt}\left[\frac{\partial L}{\partial \dot{q}_1}\right] = m_3\times\left(l_2\times c_{(c\theta_2+\theta_3)}+l_1\times c_{\theta_2}+\left(l_3\times c_{(\theta_2+\theta_3+\theta_4)}\right)/2\right)^2\times$$
$$\ddot{\theta}_1+w_c\times\left(l_2\times c_{(\theta_2+\theta_3)}+l_1\times c_{\theta_2}+l_3\times c_{(\theta_2+\theta_3+\theta_4)}\right)^2\times\ddot{\theta}_1+m_b\times r^2\times\ddot{\theta}_1+$$
$$\left(m_2\times\left(l_2\times c_{(\theta_2+\theta_3)}+2\times l_1\times c_{\theta_2}\right)^2\times\ddot{\theta}_1\right)/4+\left(l_1^2\times m_1\times c_{\theta_2}^2\times\ddot{\theta}_1\right)/4-m_2\times$$
$$\dot{\theta}_1\times\left(\left(l_2\times s_{(\theta_2+\theta_3)}\times\left(\dot{\theta}_2+\dot{\theta}_3\right)+2\times l_1\times s_{\theta_2}\times\dot{\theta}_2\right)\times\left(2\times l_1\times c_{\theta_2}+l_2\times c_{(\theta_2+\theta_3)}\right)\right)/$$
$$2-2\times m_3\times\dot{\theta}_1\times\left(l_1\times c_{\theta_2}+\left(l_3\times c_{(\theta_2+\theta_3+\theta_4)}\right)/2+l_2\times c_{(\theta_2+\theta_3)}\right)\times$$
$$\left(l_2\times s_{(\theta_2+\theta_3)}\times\left(\dot{\theta}_2+\dot{\theta}_3\right)+l_1\times s_{\theta_2}\times\dot{\theta}_2+\left(l_3\times s_{(\theta_2+\theta_3+\theta_4)}\times\left(\dot{\theta}_2+\dot{\theta}_3+\dot{\theta}_4\right)\right)/2\right)-$$
$$2\times w_c\times\dot{\theta}_1\times\left(l_1\times c_{\theta_2}+l_3\times c_{(\theta_2+\theta_3+\theta_4)}+l_2\times c_{(\theta_2+\theta_3)}\right)\times$$
$$\begin{pmatrix} l_2\times s_{(\theta_2+\theta_3)}\times\left(\dot{\theta}_2+\dot{\theta}_3\right)+l_1\times s_{\theta_2}\times\dot{\theta}_2+ \\ l_3\times s_{(\theta_2+\theta_3+\theta_4)}\times\left(\dot{\theta}_2+\dot{\theta}_3+\dot{\theta}_4\right)\end{pmatrix}-\left(l_1^2\times m_1\times c_{\theta_2}\times s_{\theta_2}\times\dot{\theta}_1\times\dot{\theta}_2\right)/2 \quad (33)$$

$$\frac{\partial L}{\partial q_1} = 0 \quad (34)$$

The same procedure is performed for the other generalized coordinates. Once the manipulator model is obtained for the first four degrees of freedom, the equations must be organized as shown in Eq. 35 where the viscous frictions are considered as a constant of friction v proportional to the generalized variable $\dot{q}$:

$$M(q)\ddot{q}+V(q,\dot{q})+G(q)+F_v\dot{q} = \tau \quad (35)$$

Where:

M(q) = The inertial matrix
$v_{(q,\dot{q})}$ = The vector of centrifugal and Coriolis forces
G(p) = The vector of gravitational forces
$\dot{q}$ = The vector of friction forces

For ease in implementing a subsequent control, Eq. 35 should be expressed as shown in Eq. 36:

$$\begin{bmatrix}\tau_1\\ \tau_2\\ \tau_3\\ \tau_4\end{bmatrix} = \begin{bmatrix} A & B & C & D\\ E & F & G & H\\ I & J & K & L\\ M & N & O & P\end{bmatrix}\begin{bmatrix}\ddot{\theta}_1\\ \ddot{\theta}_2\\ \ddot{\theta}_3\\ \ddot{\theta}_4\end{bmatrix}+\begin{bmatrix}Q\\ R\\ S\\ T\end{bmatrix}+\begin{bmatrix}U\\ V\\ W\\ X\end{bmatrix}+$$
$$\begin{bmatrix} v_1 & 0 & 0 & 0\\ 0 & v_2 & 0 & 0\\ 0 & 0 & v_3 & 0\\ 0 & 0 & 0 & v_4\end{bmatrix}+\begin{bmatrix}\dot{\theta}_1\\ \dot{\theta}_2\\ \dot{\theta}_3\\ \dot{\theta}_4\end{bmatrix} \quad (36)$$

From Eq. 36, we have for the joint 1, the torque defined by Eq. 37:

$$\tau_1 = A\ddot{\theta}_1+B\ddot{\theta}_2+C\ddot{\theta}_3+D\ddot{\theta}_4+Q+U+Fv_1\dot{\theta}_1 \quad (37)$$

where, A, B, C, D, Q, U are defined by Eq. 38-43, respectively and are obtained from the Lagrangian obtained in Eq. 32-34:

$$A = m_3\times\left(l_2\times c_{(\theta_2+\theta_3)}+l_1\times c_{\theta_2}+\left(l_3\times c_{(\theta_2+\theta_3+\theta_4)}\right)/2\right)^2+$$
$$w_c\times\left(l_2\times c_{(\theta_2+\theta_3)}+l_1\times c_{\theta_2}+l_3\times c_{(\theta_2+\theta_3+\theta_4)}\right)^2+m_b\times r^2+ \quad (38)$$
$$\left(m_2\times\left(l_2\times c_{\theta_2}+2\times l_1\times c_{\theta_2}\right)^2\right)/4+\left(l_1^2\times m_1\times c_{\theta_2}^2\right)/4$$

$$B = 0 \quad (39)$$

$$C = 0 \quad (40)$$

$$D = 0 \quad (41)$$

$$Q = -\left(m_2\times\dot{\theta}_1\times\left(2\times l_1\times\dot{\theta}_2\times s_{\theta_2}+l_2\times s_{(\theta_2+\theta_3)}\times\left(\dot{\theta}_2+\dot{\theta}_3\right)\right)\times\right.$$
$$\left.\left(l_2\times c_{(\theta_2+\theta_3)}+2\times l_1\times c_{\theta_2}\right)\right)/2-2\times m_3\times\dot{\theta}_1\times\left(l_1\times\dot{\theta}_2\times c_{\theta_2}+\right.$$
$$\left.\left(l_3\times s_{(\theta_2+\theta_3+\theta_4)}\times\left(\dot{\theta}_2+\dot{\theta}_3+\dot{\theta}_4\right)\right)/2+l_2\times s_{(\theta_2+\theta_3)}\times\left(\dot{\theta}_2+\dot{\theta}_3\right)\right)\times$$
$$\left(l_2\times c_{(\theta_2+\theta_3)}+l_1\times c_{\theta_2}+\left(l_3\times c_{(\theta_2+\theta_3+\theta_4)}\right)/2\right)-2\times\dot{\theta}_1\times w_c\times \quad (42)$$
$$\left(l_1\times\dot{\theta}_2\times s_{\theta_2}+l_3\times s_{(\theta_2+\theta_3+\theta_4)}\times\left(\dot{\theta}_2+\dot{\theta}_3+\dot{\theta}_4\right)+l_2\times s_{(\theta_2+\theta_3)}\times\right.$$
$$\left.\left(\dot{\theta}_2+\dot{\theta}_3\right)\right)\times\left(l_2\times c_{(\theta_2+\theta_3)}+l_1\times c_{\theta_2}+l_3\times c_{(\theta_2+\theta_3+\theta_4)}\right)-$$
$$\left(l_1^2\times m_1\times\dot{\theta}_1+\dot{\theta}_2\times c_{\theta_2}\times s_{\theta_2}\right)$$

$$U = 0 \quad (43)$$

**Direct dynamics:** The direct dynamic model shows the temporal evolution of the articular coordinates as well as their derivatives as a function of the forces and pairs involved. To obtain it, the inverse model of Eq. 36 to which Cramer's rule is applied and the substitution of the null Cofactors is used. For the management of the matrices in the calculation of the determinants the Eq. 44 is used. Therefore, in solving Cramer's rule we have the Eq. 45-48:

$$\begin{aligned} Z_1 &= A\ddot{\theta}_1\\ Z_2 &= F\ddot{\theta}_2+G\ddot{\theta}_3+H\ddot{\theta}_4\\ Z_3 &= J\ddot{\theta}_2+K\ddot{\theta}_3+L\ddot{\theta}_4\\ Z_4 &= N\ddot{\theta}_2+O\ddot{\theta}_3+P\ddot{\theta}_4\end{aligned} \quad (44)$$

$$\ddot{\theta}_1 = \frac{\begin{bmatrix} Z_1 & 0 & 0 & 0 \\ Z_2 & F & G & H \\ Z_3 & J & K & L \\ Z_4 & N & O & P \end{bmatrix}}{\begin{bmatrix} A & 0 & 0 & 0 \\ 0 & F & G & H \\ 0 & J & K & L \\ 0 & N & O & P \end{bmatrix}} = \frac{Z_1}{A} \quad (45)$$

$$\ddot{\theta}_2 = \frac{\begin{bmatrix} A & Z_1 & 0 & 0 \\ 0 & Z_2 & G & H \\ 0 & Z_3 & K & L \\ 0 & Z_4 & O & P \end{bmatrix}}{\begin{bmatrix} A & 0 & 0 & 0 \\ 0 & F & G & H \\ 0 & J & K & L \\ 0 & N & O & P \end{bmatrix}} = \frac{\begin{pmatrix} GLZ_4\text{-}HKZ_4\text{-}HOZ_3 + \\ HOZ_3\text{+}KPZ_2\text{-}LOZ_2 \end{pmatrix}}{\begin{pmatrix} FKP\text{-}GJP\text{+}GLN\text{-} \\ HKN\text{-}FLO\text{+}HJO \end{pmatrix}} \quad (46)$$

$$\ddot{\theta}_3 = \frac{\begin{bmatrix} A & 0 & Z_1 & 0 \\ 0 & F & Z_2 & H \\ 0 & J & Z_3 & L \\ 0 & N & Z_4 & P \end{bmatrix}}{\begin{bmatrix} A & 0 & 0 & 0 \\ 0 & F & G & H \\ 0 & J & K & L \\ 0 & N & O & P \end{bmatrix}} = \frac{\begin{pmatrix} FLZ_4\text{-}HJZ_4\text{-}FPZ_3 + \\ HNZ_3\text{+}JPZ_2\text{-}LNZ_2 \end{pmatrix}}{\begin{pmatrix} FKP\text{-}GJP\text{+}GLN\text{-} \\ HKN\text{-}FLO\text{+}HJO \end{pmatrix}} \quad (47)$$

$$\ddot{\theta}_4 = \frac{\begin{bmatrix} A & 0 & 0 & Z_1 \\ 0 & F & G & Z_2 \\ 0 & J & K & Z_3 \\ 0 & N & O & Z_4 \end{bmatrix}}{\begin{bmatrix} A & 0 & 0 & 0 \\ 0 & F & G & H \\ 0 & J & K & L \\ 0 & N & O & P \end{bmatrix}} = \frac{\begin{pmatrix} FKZ_4\text{-}GJZ_4\text{+}GNZ_3\text{-} \\ FOZ_3\text{-}KNZ_2\text{+}JOZ_2 \end{pmatrix}}{\begin{pmatrix} FKP\text{-}GJP\text{+}GLN\text{-} \\ HKN\text{-}FLO\text{+}HJO \end{pmatrix}} \quad (48)$$

**Mobile robots dynamics:** It is considered the initial structure of Fig. 4 which specifies the wheel configuration as well as the initial variables that should be considered for the development of the dynamics of the system.

To simplify the model, we consider the torques generated by the wheels located on the right as a single general torque, the same for the wheels located on the left side of the vehicle as shown in Eq. 49 (Krzystof and Dariusz, 2004).

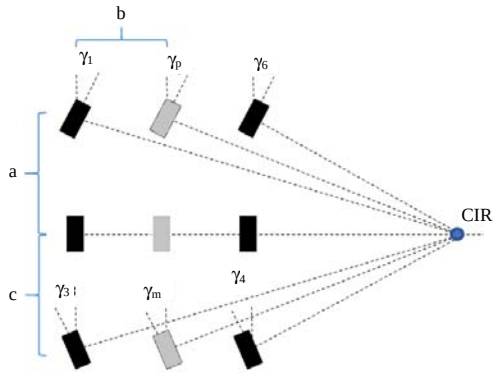


Fig. 4: Six-wheel robotic platform

$$\tau = \begin{bmatrix} \tau_L \\ \tau_R \end{bmatrix} = \begin{bmatrix} \tau_1 + \tau_2 + \tau_3 \\ \tau_4 + \tau_5 + \tau_6 \end{bmatrix} \quad (49)$$

From the Eq. 49, we specify the generalized coordinates that characterize the movement of the system from which we obtain three variables that describe the position and orientation of the platform and two variables that specify the angular positions of the wheels which the coordinates of Lagrange are presented in Eq. 50:

$$q = (x_c, y_c, \theta, \varphi_R, \varphi_L) \quad (50)$$

where, $x_c$ and $y_c$ represent the coordinates of the center of mass of the platform $\theta$ is the orientation angle of the system and $\varphi_i$. The angular position of the vehicle wheels.

**Inverse dynamics:** For the development of the inverse dynamics of the hybrid platform, the Euler-Lagrange formalism is implemented which can be described by Eq. 51 (Dhaouadi and Hatab, 2013):

$$M(q)\ddot{q}+V(q,\dot{q})\dot{q}+F_v\dot{q} = B(q)\tau\text{-}A^T(q)\lambda$$

Where:

$A^T(q)$ = The Jacobian matrix of movement restrictions

$\lambda$ = The vector of force constraints or lagrange multipliers

This scheme, it's like the one proposed in the dynamic equation of a robot manipulator. The differences are found in the right part of the equation where two facts are considered exclusive to mobile robots: not all wheels have to be actuated, besides there are non-holonomic constraints to robot movement.

To begin with the development of the mathematical model, the movement restrictions under which the system

is subjected are presented. The first in Eq. 52, defines that the vehicle cannot be moved sideways, only forwards and backwards, this means that the linear speed of the mechanism is governed by the linear velocity of each wheel defined in turn by its the angular velocity (Tian *et al*., 2009):

$$\dot{y}_c c_\theta - \dot{x}_c s_\theta = 0 \tag{52}$$

The other restrictions present are shown in Eq. 53 and correspond to the rolling and non-displacement conditions of the vehicle's traction wheels. Where $\theta_i$ is defined as the distance between the center of the vehicle and the traction side wheels:

$$\begin{aligned} \dot{x}_c c_\theta + \dot{y}_c s_\theta + l\dot{\theta} &= r\dot{\varphi}_R \\ \dot{x}_c c_\theta + \dot{y}_c s_\theta - l\dot{\theta} &= r\dot{\varphi}_L \end{aligned} \tag{53}$$

The trictions specified above can be written as $A(q)\dot{q} = 0$, where A(q) is specified in Eq. 54 (Sarkar *et al*., 1993):

$$A(q) = \begin{bmatrix} -s_\theta & c_\theta & 0 & 0 & 0 \\ -c_\theta & -s_\theta & -l & r & 0 \\ -c_\theta & -s_\theta & 1 & 0 & r \end{bmatrix} \tag{54}$$

Now, we proceed by deriving the dynamic equations of the mobile platform, so that the Lagrange equations with the Lagrange multipliers $\lambda_c$, $\lambda_R$, $\lambda_L$ are given by Eq. 55:

$$\begin{aligned} &m\ddot{x}_c - \lambda_c s_\theta - (\lambda_R + \lambda_L) c_\theta = 0 \\ &m\ddot{y}_c + \lambda_c c_\theta - (\lambda_R + \lambda_L) s_\theta = 0 \\ &I_{\ddot{\theta}} + l\lambda_R + l\lambda_L = 0 \\ &I_1\ddot{\varphi}_R + \lambda_R r = \tau_R \\ &I_2\ddot{\varphi}_L + \lambda_L r = \tau_L \end{aligned} \tag{55}$$

where, $m = m_c + 2m_r$ to $m_r$ equal to the wheels mass and $m_c$ equal to the vehicle mass without the wheels; $I = I_c + 2I_i$, for $I_c = (1/2) \times m_c \times r^2$ defined as the moment of inertia of the mobile and $\tau$ the moment of inertia of the wheels which for this case study can be taken as the same value for all and $\tau_i$ which is specified as the torque acting on the axle of the wheels (Yun and Yamamoto, 1993). Finally, to obtain Eq. 52, we proceed to define the matrices that characterize it, as shown in Eq. 56-59:

$$M(q) = \begin{bmatrix} m & 0 & 0 \\ 0 & m & 0 \\ 0 & 0 & I \end{bmatrix} \tag{56}$$

$$V(q, \dot{q}) = \begin{bmatrix} 0 \\ 0 \\ 0 \end{bmatrix} \tag{57}$$

$$B(q) = \frac{1}{r} \begin{bmatrix} c_\theta & c_\theta \\ s_\theta & s_\theta \\ 1 & -l \end{bmatrix} \tag{58}$$

$$\tau = \begin{bmatrix} \tau_R \\ \tau_L \end{bmatrix} \tag{59}$$

Then, we define the matrix S(q) of Eq. 60 formed by a set of linearly independent vectors that span the null space of A(q). Therefore, the multiplication of these matrices is defined as Eq. 61:

$$S(q) = \begin{bmatrix} \left(\frac{r}{2l}\right) l \times c_\theta & \left(\frac{r}{2l}\right) l \times c_\theta \\ \left(\frac{r}{2l}\right) l \times s_\theta & \left(\frac{r}{2l}\right) l \times s_\theta \\ \frac{r}{2l} & -\frac{r}{2l} \end{bmatrix} \tag{60}$$

$$S(q)^T A^T(q) = 0$$

In addition, it is possible to find a vector of time functions for all t, defined as $v(t) = [v_R\ v_L]$ which represent the angular velocities of the wheels on the right and left of the vehicle and allow obtaining $\dot{q}(t) = S(q)v(t)$ in Eq. 62, whereby lagrange multipliers can be eliminated from the general dynamics equation (Mehrjerdi and Saad, 2010):

$$\begin{bmatrix} \dot{x}_c \\ \dot{y}_c \\ \dot{\theta} \end{bmatrix} = \begin{bmatrix} \left(\frac{r}{2l}\right) l \times c_\theta & \left(\frac{r}{2l}\right) l \times c_\theta \\ \left(\frac{r}{2l}\right) l \times s_\theta & \left(\frac{r}{2l}\right) l \times s_\theta \\ \frac{r}{2l} & -\frac{r}{2l} \end{bmatrix} \begin{bmatrix} v_R \\ v_L \end{bmatrix} \tag{62}$$

$$\begin{bmatrix} v_R \\ v_L \end{bmatrix} = \begin{bmatrix} \frac{1}{r} & \frac{1}{r} \\ \frac{1}{r} & \frac{1}{r} \end{bmatrix} \begin{bmatrix} v \\ w \end{bmatrix}$$

Annex, this expression can be differentiable until we obtain Eq. 63, cleared in Eq. 64:

$$\ddot{q}(t) = \dot{S}(q)v(t) + S(q)\dot{v}(t) \tag{63}$$

$$\begin{bmatrix}\ddot{x}_c\\ \ddot{y}_c\\ \ddot{\theta}\end{bmatrix}=\begin{bmatrix}-\dot{\theta}\times s_\theta & 0\\ \dot{\theta}\times c_\theta & 0\\ 0 & 0\end{bmatrix}\begin{bmatrix}v\\ w\end{bmatrix}+\begin{bmatrix}s_\theta & 0\\ c_\theta & 0\\ 0 & 0\end{bmatrix}\begin{bmatrix}\dot{v}\\ \dot{w}\end{bmatrix}$$
$$\begin{bmatrix}\ddot{x}_c\\ \ddot{y}_c\\ \ddot{\theta}\end{bmatrix}=\begin{bmatrix}-\dot{\theta}\times v\times s_\theta+\dot{v}\times c_\theta\\ \dot{v}\times s_\theta-\dot{\theta}\times v\times c_\theta\\ \dot{w}\end{bmatrix} \quad (64)$$

From Eq. 51, the dynamics can be re-structured as shown in Eq. 65:

$$\begin{bmatrix}m & 0 & 0\\ 0 & m & 0\\ 0 & 0 & I\end{bmatrix}\ddot{q}=\frac{1}{r}\begin{bmatrix}c_\theta & c_\theta\\ s_\theta & s_\theta\\ 1 & -1\end{bmatrix}\begin{bmatrix}\tau_R\\ \tau_L\end{bmatrix}+\begin{bmatrix}s_\theta\\ -c_\theta\\ 0\end{bmatrix}\lambda \quad (65)$$

From Eq. 64 and 65, one can conclude the values of $\dot{v}$ and $\dot{w}$ as shown in Eq. 66 and 67:

$$\dot{v}=\frac{(\tau_R+\tau_L)}{m\times r} \quad (66)$$

$$\dot{v}=\frac{1\times(\tau_R+\tau_L)}{I\times r} \quad (67)$$

Multiplying Eq. 60 with Eq. 51, we obtain Eq. 68 to be implemented as shown in Eq. 69 (Williams *et al*., 2002):

$$\begin{aligned}&S(q)^T M(q)\ddot{q}+S(q)^T V(q,\dot{q})\dot{q}+S(q)^T\\ &F_v\dot{q}=S(q)^T B(q)\tau-S(q)^T A^T(q)\lambda\end{aligned} \quad (68)$$

$$\ddot{q}=\left(S(q)^T M(q)\right)^{-1}\begin{pmatrix}-S(q)^T V(q,\dot{q})\dot{q}-S(q)^T\\ F_v\dot{q}+S(q)^T B(q)\tau\end{pmatrix} \quad (69)$$

## RESULTS AND DISCUSSION

**Manipulator results:** The system dynamics simulation is performed with torques and pulse signals of amplitude 2 N/m and a period of 5 sec which it is observed if the angles of Fig. 5 and velocities of Fig. 6 have constant behaviors with values that do not tend to infinity.

**Mobile platform results:** To verify the correct calculation of the dynamic difference of the mobile robot, we considered (Fig. 7) which shows the angular variation of a vehicle based on the changes of radius of Fig. 8 that are determined by the instantaneous center of rotation in a random path.

From the results obtained in radius and angle the simulation is performed having as input torques with amplitude of 10 N/m which a constant behavior in speed in is observed with variations in Y given by the angular changes in the direction of the vehicle as shown in Fig. 5. The value of $\theta$ is due to an initial condition specified as a value of 0.7854.

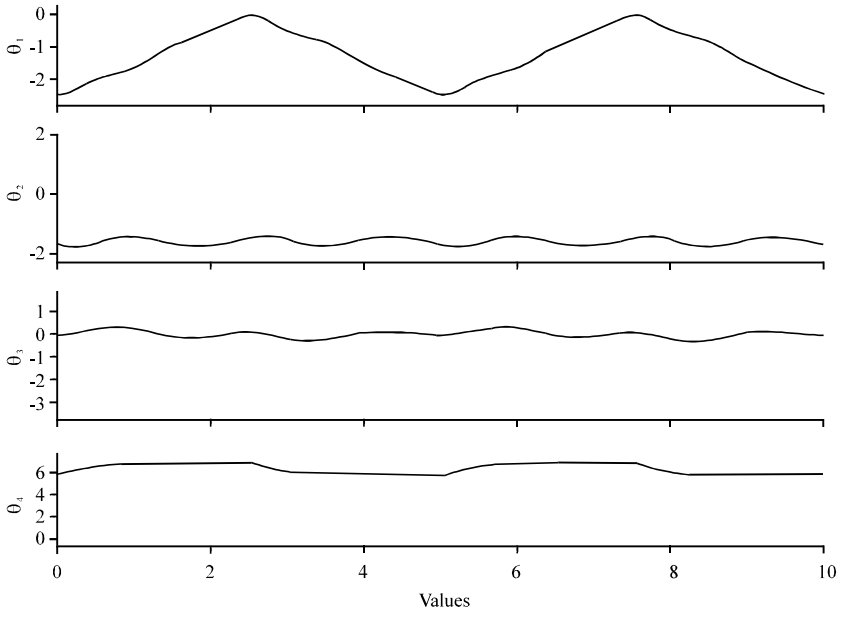


Fig. 5: Angular behavior of the joints

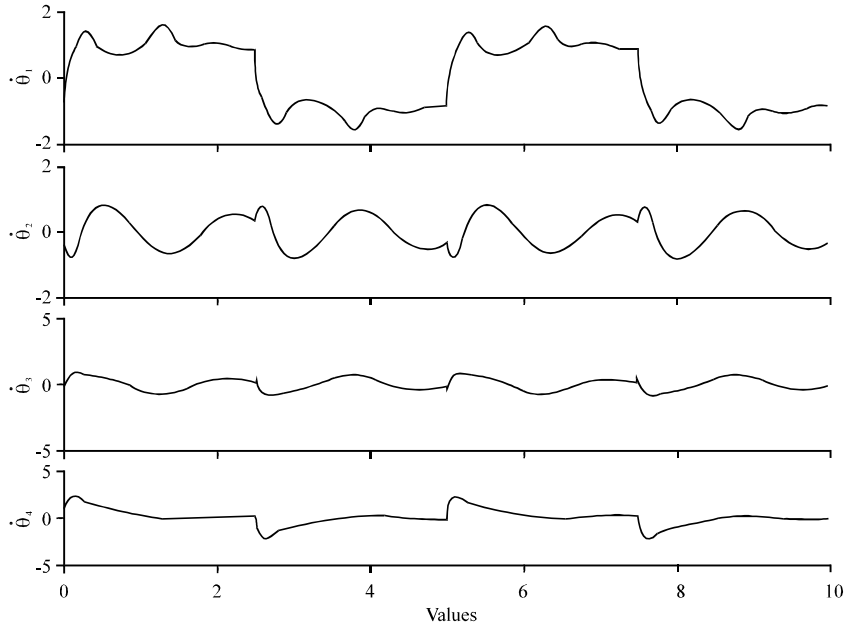


Fig. 6: Velocity behavior of the joints

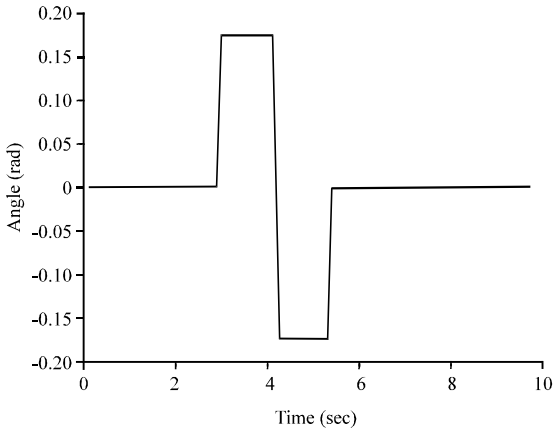


Fig. 7: Angular trajectory

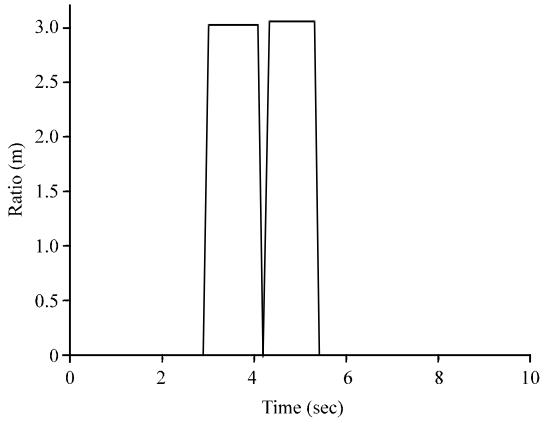


Fig. 8: Radio for calculation of inertia

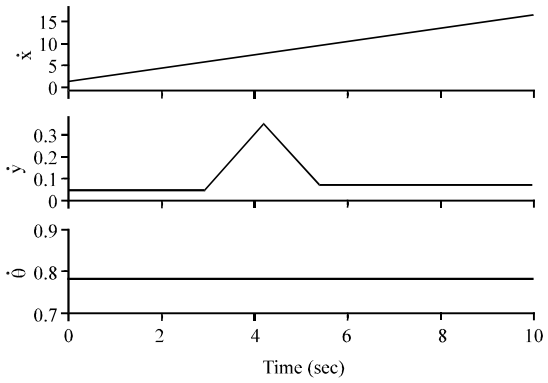


Fig. 9: Behavior in velocity of the generalized coordinates of the mobile robot

## CONCLUSION

When performing the simulations in the manipulator, it was verified that none of the behaviors of generalized coordinates nor their derivatives have values that tend to infinity which ensures the correct calculation of the dynamics of the mechanism. On the other hand, when performing the mobile platform simulations, it was verified that none of the behaviors of the generalized coordinates nor their derivatives have values that tend to infinity which ensures the correct calculation of the dynamics of the mechanism.

With the calculation made, it is possible to proceed with the implementation of control algorithms that allow

to obtain the desired behaviors in the system when performing trajectories in addition to ensuring that none of the torques exceeds the maximum value of the motors.

## ACKNOWLEDGEMENT

The research for this study was supported by Militar Nueva Granada University, through the project ING-IMP-2138.

## REFERENCES

Campion, G., G. Bastin and B. D'Andrea-Novel, 1996. Structural properties and classification of kinematic and dynamic models of wheeled mobile robots. IEEE Trans. Robotics Automation, 2: 47-62.

Craige, J.J., 1989. Introduction to Robotics Mechanics and Control. 2nd Edn., Addison-Wesley, Redwood City, CA., ISBN: 0201095289.

Dhaouadi, R. and A.A. Hatab, 2013. Dynamic modelling of differential-drive mobile robots using lagrange and newton-euler methodologies: A unified framework. Adv. Robot. Autom., 2: 1-7.

Jones, J.L., B.A. Seiger and A.M. Flynn, 1993. Mobile Robots: Inspiration to Implementation. A.K. Peters, Natick, Massachusetts, ISBN:9781568810119, Pages: 349.

Krzystof, K. and P. Dariusz, 2004. Modeling and control of a 4 wheel skid-steering mobile robot. Int. J. Applied Math. Comput. Sci., 14: 477-496.

Mehrjerdi, H. and M. Saad, 2010. Dynamic tracking control of mobile robot using exponential sliding mode. Proceedings of the 36th Annual IEEE Conference on Industrial Electronics Society, November 7-10, 2010, IEEE, Glendale, Arizona, ISBN:978-1-4244-5225-5, pp: 1517-1521.

Ogata, K., 1987. Systems Dynamic. Prentice Hall, Upper Saddle River, New Jersey, USA.,.

Sarkar, N., X. Yun and V. Kumar, 1993. Dynamic path following: A new control algorithm for mobile robots. Proceedings of the 32nd IEEE Conference on Decision and Control, December 15-17, 1993, IEEE, San Antonio, Texas, ISBN:0-7803-1298-8, pp: 2670-2675.

Tian, Y., N. Sidek and N. Sarkar, 2009. Modeling and control of a nonholonomic wheeled mobile robot with wheel slip dynamics. Proceedings of the IEEE Symposium on Computational Intelligence in Control and Automation, March 30-April 2, 2009, IEEE, Nashville, Tennessee, ISBN:978-1-4244-2752-9, pp: 7-14.

Williams, R.L., B.E. Carter, P. Gallina and G. Rosati, 2002. Dynamic model with slip for wheeled omnidirectional robots. IEEE. Trans. Rob. Autom., 18: 285-293.

Yun, X. and Y. Yamamoto, 1993. Internal dynamics of a wheeled mobile robot. Proceedings of the IEEE/RSJ International Conference on Intelligent Robots and Systems IROS'93, July 26-30, 1993, IEEE, Yokohama, Japan, ISBN:0-7803-0823-9, pp: 1288-1294.

Zhao, Y. and S.L. Bement, 1992. Kinematics, dynamics and control of wheeled mobile robots. Proceedings of the Conference on Robotics and Automation, May 12-14, 1992, Nice, France, pp: 91-96.